Detailed Report

The project has maintained its focus on nucleocytoplasmic abnormalities in neurodegenerative TDP-43 proteinopathies. However, there have been substantial changes regarding the focus on investigated proteins. The pandemic has led to slowdowns and adjustments in work. Due to the PIs change in work schedule and affiliation, both funding and staff employment has been covered by external sources (incl. PI`s research support funds at KCL), which led to substantial underspending of the grant`s budget. The Recipient Institution (SZTE) shall return the unspent funds to the Funding Agency (see Financial Report).

For the research carried out within the project, we selected post-mortem cases from TDP-43 positive subtypes of frontotemporal dementia (FTD/ALS-TDP) and motoneuron disease (MND/ALS): sporadic ALS/FTD, C9ORF72 mutant 'C9ALS/FTD', for which age-matched controls were selected for comparison. Over more than a decade of research collaboration, we recruited well-characterized cases from the London Brain Bank. The role of the KPNA4 protein in nucleocytoplasmic transport of TDP-43 was investigated using several methods. Neuropathological examination by Western blot confirmed down-regulation of soluble KPNA4 and histological nuclear depletion and cytoplasmic mislocalisation, which was also statistically confirmed. In the Drosophila model, we found corresponding results for the human homologous proteins, and confirmed that TDP-43 causes karyopherin dysfunction (and not vice versa), with a pathological feedback mechanism that recruits KPNA4 (or Drosophila-homologous Importin-alpha3) function by its modification to partially restore the normal distribution of TDP-43 in the nucleus and cytoplasm. A second nucleo-cytoplasmic transport protein, KPNA3, was examined neuropathologically in control and neurodegenerative cases (also investigating different types of alpha-synucleinopathies), altering the nucleus-cytoplasm ratio. The CAS/CSE1L immunohistochemistry was performed with two different antibodies (both Santa Cruz) and different dilutions, and sections were digitized. Contrary to expectations, in many cases the labelling is very weak or of questionable specificity, so we have put more emphasis on the investigation of the KPNA4, KPNAB, and KPNA3 transporter proteins in collaboration with the Slovenian partner (BR), which has yielded publishable results in high impact journals.

The majority of the results will be submitted to a Q1/D1 journal by the end of 2023. (For details, see Subheading 2).

Our results are presented and discussed below under four subheadings, arranged according to the respective topic and manuscript/publication.

1. **Karyopherin abnormalities in neurodegenerative proteinopathies** (Pasha T., Zatorska A., Sharipov D., Rogelj B., Hortobágyi T., Hirth F.: Karyopherin abnormalities in neurodegenerative proteinopathies.). **Classification, pathogenetic and therapeutic implications** (See paper 6 in the publication list below)

The authors are: my MSc students (TP, AZ), PhD student (DS), co-supervisor (FH), and the Slovenian co-PI (BR) on this bilaterally funded (NKFIH-SNN/ARRS) project.

The aberrant nucleocytoplasmic transport is a major area of neurodegeneration research. This paper focuses on abnormalities of Karyopherin proteins (which are highly important in nucleocytoplasmic transport) in frontotemporal dementias (especially FTD-TDP) and ALS,

complemented and compared with Alzheimer's disease, FTD-tau, synucleinopathies and Huntington's disease. The importance of Karyopherin-beta (KPNB) and CAS/CSE1L have been highlighted. We believe this is an important publication in the field, which has attracted numerous citations (n=19 within less than 2 years).

Neurodegenerative proteinopathies are characterized by progressive cell loss that is preceded by the mislocalization and aberrant accumulation of proteins prone to aggregation. Despite their different physiological functions, disease-related proteins like tau, α-synuclein, TAR DNA binding protein-43, fused in sarcoma and mutant huntingtin, all share low complexity regions that can mediate their liquid-liquid phase transitions. The proteins' phase transitions can range from native monomers to soluble oligomers, liquid droplets and further to irreversible, often-mislocalized aggregates that characterize the stages and severity of neurodegenerative diseases. Recent advances into the underlying pathogenic mechanisms have associated mislocalization and aberrant accumulation of disease-related proteins with defective nucleocytoplasmic transport and its mediators called karyopherins. These studies identify karyopherin abnormalities in amyotrophic lateral sclerosis, frontotemporal dementia, Alzheimer's disease, and synucleinopathies including Parkinson's disease and dementia with Lewy bodies, that range from altered expression levels to the subcellular mislocalization and aggregation of karyopherin α and β proteins. The reported findings reveal that in addition to their classical function in nuclear import and export, karyopherins can also act as chaperones by shielding aggregation-prone proteins against misfolding, accumulation and irreversible phase-transition into insoluble aggregates. Karyopherin abnormalities can, therefore, be both the cause and consequence of protein mislocalization and aggregate formation in degenerative proteinopathies. The resulting vicious feedback cycle of karyopherin pathology and proteinopathy identifies karyopherin abnormalities as a common denominator of onset and progression of neurodegenerative disease. Pharmacological targeting of karyopherins, already in clinical trials as therapeutic intervention targeting cancers such as glioblastoma and viral infections, is a promising tool for disease-modifying treatments in neurodegenerative proteinopathies.

2. **A Pathogenic Feedback Loop between TDP-43 and Karyopherin-α4 in neurodegenerative TDP-43 proteinopathy** (See paper 3 in the publication list)

Background

Frontotemporal dementia (FTD) shares with Amyotrophic lateral sclerosis (ALS) several clinico-pathological features[4,5], including the accumulation and aggregation of aberrant, intracellular inclusions of TAR DNA-binding protein 43 (TDP-43)[6,7] that are found in 97% of ALS and 45% of FTD cases[8].

Cytoplasmic TDP-43 inclusions concur with its nuclear depletion, suggesting a cellular state whereby both nuclear loss and cytoplasmic gain of TDP-43 function contribute to disease onset and progression[10]. Indeed, targeted cytoplasmic accumulation of TDP-43 has been shown to induce its nuclear depletion and aggregate formation which have been directly related to onset and progression of disease[15-18].

TDP-43 pathology is associated with almost all cases of ALS/FTD characterised by a hexanucleotide GGGGCC (G_4C_2) repeat expansion in intron 1 of chromosome 9 open reading frame 72 (*C9ORF72*), the most common genetic cause of ALS and FTD (C9ALS/FTD)[19-21]. Several studies identified defective nucleocytoplasmic transport (NCT) and nuclear pore complex (NPC) deficits as critical events in C9ALS/FTD[23-26], including pathological abnormalities of nuclear transport receptors termed karyopherins[18,23,25,27,28].

Karyopherins (also referred to as importins or exportins) are classified into alpha (KPNA) and beta (KPNB) families, with KPNAs mediating cargo transport across the nuclear membrane through NLS recognition of cargo proteins[29]. KPNAs interact with TDP-43[23,27,30], with KPNA3 and KPNA4 exhibiting the strongest interactions[30]. In addition to their role in nucleocytoplasmic transport, karyopherins have been recognised for their functions as molecular chaperones and disaggregases[31-33]. Moreover, karyopherin abnormalities such as disrupted karyopherin-binding have been shown to disturb TDP-43 nucleocytoplasmic transport and have been implicated in TDP-43 pathology[10]. While these studies established a direct link between TDP-43 pathology and KPNA4 phenotypes in FTD, it has remained elusive whether such abnormalities also characterise ALS and whether these are the cause or consequence of TDP-43 pathology.

Here we show the downregulation of soluble KPNA4, as well as the cytoplasmic redistribution and mislocalisation of KPNA4 in post-mortem spinal cord of sporadic ALS and C9ALS cases that are characterised by TDP-43 pathology. Using *Drosophila*, we demonstrate that targeted accumulation of KPNA4 was insufficient in causing TDP pathology. In contrast, targeted cytosolic accumulation of *Drosophila* TDP-43 caused KPNA4 pathologies including its nuclear decrease and cytoplasmic accumulation. Moreover, we demonstrate that overexpression of KPNA4 in the presence of accumulating cytoplasmic TDP43 leads to a partial nuclear rescue and restoration of both TDP-43 and KPNA4 itself. These findings establish KPNA4 abnormalities in ALS spinal cord and demonstrate in *Drosophila* their functional interaction with accumulating TDP-43, suggesting a feedback loop between TDP-43 and KPNA dysfunction that directly contributes to the onset and progression of disease.

Materials and methods

Human post-mortem tissue

Human post-mortem samples were provided by the London Neurodegenerative Diseases Brain Bank (King's College London, UK), where the PI (TH) has had research and diagnostic collaboration for more than a decade. Consent for autopsy, neuropathological assessment and research was obtained for all donors and all studies were carried out under the ethical approval of the tissue bank (08/MRE09/38+5 and 18/WA/0206). Block taking for histological and immunohistochemical analyses and neuropathological assessment of sALS (n=8), C9ALS (n=9) and control (n=5) cases was performed in accordance with published guidelines[34]. Control cases were defined as age matched subjects with no clinical history or neuropathological evidence of a neurodegenerative condition (showing age-related pathology only) (case list can be provided upon request). All sALS cases showed typical TDP-43 pathology in the form of neuronal cytoplasmic inclusions and additional glial inclusions in some cases. The C9ALS cases had all previously undergone repeat primed PCR to identify the repeat expansion, and all showed the characteristic TDP-43 and p62 pathology associated with C9ORF72 expansion[35].

Human post-mortem tissue Western Blotting

Samples were homogenised in lysis buffer (100 mg/ml) consisting of RIPA buffer (89901, Thermo Fisher Scientific) supplemented with 1X protease inhibitors (78430, Thermo Fisher Scientific) and 1X phosphatase inhibitors (524625-1SET, MERCK). Total homogenate was spun at 12000 g for 10 minutes and supernatant collected diluted 1:4 to form a working concentration stored at -80ºC. Post-Mortem tissue supernatant was thawed on ice for 20 minutes before vortexing and total protein concertation determination using a Pierce BCA assay (23225, Thermo Fisher Scientific). Samples were normalised to the lowest protein concentration using lysis buffer, and loading buffer (928-40004, Li-Cor) and DTT (10 mM final concentration) were added. Samples were then boiled at 95 degrees for 7 minutes. Approximately 20 ug of

total protein were then loaded onto a 10% Bis-Tris gel (WG1202BOX, Thermo Fisher Scientific) and then ran using MES buffer (NP0002, Thermo Fisher Scientific) at 120V for 100 minutes. Gels were washed in dH2O and transfer buffer (BT0006, Thermo Fisher Scientific) before transferring to a nitrocellulose membrane stack (IB23002, Thermo Fisher Scientific) and transferred using an iBlot2 program P0. The nitrocellulose membrane was then washed with dH2O and blocked for 1 hour at room temperature in 3% BSA in Tris Buffer + 0.1% Tween (TBST). Membranes were incubated overnight at 4ºC in 1 ug/ml goat anti-KPNα -4 (ab6039, Abcam) then were washed with TBST before incubation for 1 hour at room temperature in Donkey anti-Goat 680 secondary antibody (1:5000; 926-68074, Li-Cor). Membranes were then incubated at room temperature for 1 hour with Rabbit anti-β-actin (1:1000; ab8227, Abcam) followed by washing and incubation with Donkey anti-rabbit 800 secondary antibody (1:5000; 926-32213, Li-Cor). Membranes were imaged using an LiCor Odyssey Clx. Quantification of images was performed on ImageStudio. Anomalies were removed if sample values were +/- 2x SD from the mean which resulted in sample 5 from the sporadic group being removed from analysis. Sample 8 from the C9ALS cohort was removed due to large P62 inclusions resulting in greater autophagosomal activity and no bands showing for either KPNA4 or the β-actin loading control. The remaining data (n=8 control, n=7 Sporadic and n=7 C9ALS) were determined to be normally distributed using Shapiro-Wilk test for control, sporadic and C9ALS groups respectively. Ordinary one-way ANOVA with multiple comparisons was performed to determine inter group significance.

Human post-mortem tissue immunohistochemistry

For immunohistochemistry of post-mortem human spinal cord samples 7μm thick sections were prepared from formalin-fixed, paraffin–embedded tissue blocks. To perform immunostaining, paraffin was removed with xylene and sections were rehydrated in an ethanol series (99% and 95%) for 3 minutes each. Slides were then microwaved in sodium citrate buffer to enhance antigen retrieval. Non-specific binding was blocked for 20 minutes with Normal Swine Serum (NSS) (Agilent) at 1:10 in TBS. For immunohistochemistry, primary rabbit anti-KPNA4 (1:500, Novus) was added together with NSS at 1:100 in TBS and incubated overnight at 4°C. After washing with TBS, sections were incubated with biotinylated secondary antibody (Agilent) diluted 1:100 in TBS, followed by incubation with ABC HRP (Thermo Fisher Scientific) solution. Finally, sections were incubated for up to 10 minutes with 3,3′-diaminobenzidine (DAB) chromogen (Sigma-Aldrich, Dorset UK) in TBS containing 0.04% hydrogen peroxide. Sections were counterstained with Harris' haematoxylin and dehydrated in IMS and xylene. Finally, sections were coverslipped using Ralmount glue and allowed to set.

Semi-quantitative evaluation of KPNA4 pathology in human post-mortem spinal cord

Immunostaining was examined and assessed blind to diagnosis. A variety of indicators reflecting KPNA4 morphology, location and intensity were quantified and semi-quantitatively scaled using an Olympus Viewer microscope. The overall motor neuronal, cytoplasmic and nuclear staining intensity, respectively, was scored (0 - none, 1 - mild, 2 - moderate, 3 - intense); reduced nuclear staining defined as the severity of reduced neuronal nuclear staining as compared to cytoplasmic staining (no difference, mild, moderate, severe reduction).

In vivo interaction between Karyopherin-α and TDP-43

Genes for TDP43-wt and dNLS-TDP-43 were inserted into vector pcDNA3.1-myc-BioID2-MCS (Addgene, # 74223), containing coding sequence for biotin ligase (BioID2) via the *BamHI* and *KpnI* restriction sites. Myc-BioID2-TDP-43wt, myc-BioID2-dNLS-TDP-43 and myc-BioID2-MCS cassettes were cloned into pcDNA5-FRT vector for establishing Flp-In HEK293

cell lines. Cassettes were amplified from pcDNA3.1 vectors; primer sequences used for molecular cloning of constructs with BioID2 ligase can be provided upon request..

Stable Flp-In HEK293 cells containing FRT sites for the insertion of cloned pcDNA5-FRT plasmids were maintained in DMEM culture medium supplemented with 10% tetracycline-free FBS, 1% mixture of penicillin/streptomycin and 100ug/ml Zeocine (InvivoGen). The cells were grown at 37°C in a humidified atmosphere with 5% CO_2. For preparation of stable cell lines expressing recombinant fusion proteins with biotin ligase, cells were co-transfected with pcDNA5-FRT plasmids (pcDNA5-FRT-myc-BioID2 or pcDNA5-FRT-myc-BioID-TDP-43wt or pcDNA5-FRT-myc-BioID-dNLS-TDP-43) and pOG44 plasmids with Lipofectamine 2000 reagent (Invitrogen). Transfected cells were cultured for 48h before adding selection medium containing hygromycin B Gold (175 μg/mL, InvivoGen). Selection medium was changed twice per week until a resistant population was obtained.

Each Flp-In cell line (BioID2, BioID2-TDP-43wt, BioID2-TDP-43-dNLS) was seeded onto 10 cm dish. When cells reached confluence, induction medium containing 1ug/mL doxycycline and 50 uM biotin was added to the cells and they were incubated for an additional 19h. Afterwards cells were washed 3 times with PBS, scraped in PBS and washed additional 3 times. PBS was removed and 1 ml of lysis buffer (0.2% SDS, 500 mM NaCl, 1 mM DTT, 50 mM Tris-HCl (pH 7.4), protease inhibitors) was added to the cell pellet. Triton-X-100 was added to the lysates to a final concentration of 2% and samples were sonicated on ice (3x45s with 30s incubation on ice). Equal amount of 50mM tris-HCl was added to the lysates and they were centrifugated for 15 min at 16.000 rcf, 4°C. Supernatants were incubated with 100 ul streptavidin-coated magnetic beads (DynaBeads MyOne T1, Invitrogen) per lysate overnight on a rotor at 4°C.

After overnight binding to streptavidin beads several washing steps were performed: two times with buffer 1 (2% SDS, 4M urea, 150 mM NaCl) with 8 minute incubation on rotor, RT, three times with buffer 2 (0.1% deoxycholic acid, 1% Triton-X-100, 500 mM NaCl, 50 mM HEPES (pH 7.5) 1 mM EDTA), three times with buffer 3 (0.5% deoxycholic acid, 0.5% NP-40, 250 mM LiCl, 10 mM Tris-HCl (pH 7.4) 1 mM EDTA) and two times with Tris-HCl (50 mM). The beads were resuspended in 0.1% SDS loading buffer + 0.2 M DDT and boiled for 7 minutes at 95°C. Samples including HEK 293T whole lysate were loaded onto 4%-12% SDS gels and SDS-PAGE was run for 1.5h at 35mA. Proteins were transferred onto nitrocellulose membrane using semi-dry transfer (BioRad, Hercules, California, USA) programme for 1.5mm gels. Blocking was performed for 1h at RT in blocking solution (2.5% skim milk + 1% BSA in TBST). The membranes were than incubated for two days in primary antibodies diluted in blocking solution: KPNA1 (mouse, Santa Cruz Biotechnology, sc-101292, 1:750), KPNA3 (mouse, Santa Cruz Biotechnology, sc-514101, 1:750), KPNA4 (rabbit, Proteintech, 12463-AP, 1:750), KPNA6 (mouse, Santa Cruz Biotechnology, sc-390055, 1:750), KPNA7 (rabbit, GeneTex, GTX31991, 1:1000). Next day the membranes were washed 3x10 min with TBST and incubated in secondary anti-rabbit-HRP (Jackson ImmunoResearch, 111-035-045, 1:5000 in blocking solution) or anti-mouse-HRP (Jackson Immunoresearch, 115-035-068, 1:5000 in blocking solution) for 1h at RT. The membranes were washed 3x10min with TBST and incubated with Clarity Max Western ECL Substrate (Bio-Rad, Hercules, California, USA). The GelDoc System and ImageLab software (both from Bio-Rad, Hercules, California, USA) were used for image acquisition and densitometric analysis, respectively.

Drosophila stocks and genetics

All fly stocks were maintained at 25°C in a 12-h light-dark cycle on standard cornmeal food. The *UAS-Kap-α3* stock was generously provided by Herve Tricoire (Paris Diderot University)[36]. The *FKH-Gal4* stock targeting Gal4 to salivary gland cells was generously provided by Eric Baehrecke (University of Massachusetts Medical School, Worcester)[37]. The w^{1118} line was obtained from the Bloomington *Drosophila* Stock Center. The *ΔNLS-TBPH* line expresses the *Drosophila* TDP-43 homolog TAR DNA-Binding Protein-43 Homologue, TBPH[38] with a mutated nuclear localisation signal (ΔNLS) under the control of the endogenous *TBPH* promoter and has been described previously[18]. For Kap-α3 gain-of-function experiments in a disease-related background, we crossed *ΔNLS-TBPH* with *UAS-Kap-α3* lines. To ensure simultaneous expression of both genetic constructs within salivary glands, experimental strains carrying both *ΔNLS-TBPH* and *UAS-Kap-α3* were crossed with *FKH-Gal4*.

Drosophila immunohistochemistry

Salivary gland preparations were dissected and stained according to protocols previously described[39]. Briefly, tissue was dissected in cold Phosphate Buffer Sodium (PBS) (0.1M NaH_2PO_4, 0.1M Na_2HPO_4) for up to 30 minutes. Samples were then fixed in Phosphate Buffer Lysine (0.2M lysine hydrochloric acid, pH adjusted to 7.4 by addition of 0.1M Na_2HPO_4, volume adjusted to 100ml 0.1M PBS) with 8% Paraformaldehyde (PLP) mixed in a 3:1 part ratio on a rotator, for up to 1 hour at room temperature. Subsequently, samples were washed in PBS with 0.5% Triton X-100 (PBT) and then blocked for 15 minutes with freshly prepared PBT containing 10% Normal Goat Serum (NGS). Samples were then incubated overnight at 4°C with primary antibodies diluted in 10% PBT-NGS. Larval salivary glands were immunolabelled using rabbit anti-TBPH (1:2000)[38], rabbit anti-Importin-α3 (1:300, kind gift from S. Cotterill) and mouse monoclonal anti-MAB414 (1:500, Abcam). Washes with PBT preceded incubation with secondary antibodies diluted in 10% PBT-NGS for up to 3 hours, in the dark, at room temperature. Secondary antibodies conjugated to Alexa Fluor® 488 and 568 (Life Technologies) were used at a final concentration of 1:150. Finally, tissues were washed with PBT and then PBS, before being left at 4°C overnight in Vectashield with DAPI (Vector laboratories). Last, the glands were finely dissected and mounted onto a glass slide for microscopic observation.

Confocal microscopy, image acquisition and analysis

All images were obtained using a Nikon A1R confocal microscope driven by NIS-Elements AR software and equipped with a 60×, NA 1.4 objective. Identical confocal microscope setting was used when imaging both control and experimental genotypes. For quantification of the nuclear/cytoplasmic ratios, full Z-stacks were taken at 0.5 μm intervals across the plane of salivary gland cells. The nuclear region was defined by immunolabelling with the nuclei marker DAPI, and MAB414, which aided in determining TBPH/Importin-α3 localisation. Images were processed using ImageJ, with nuclear-cytoplasmic ratios established from pixel intensities that were used as a quantitative readout for protein expression either side of the nuclear membrane.

Statistical analysis

Statistical analysis was performed using GraphPad Prism 8.0. Variability of values is given as the standard error of the mean (SEM). Results are reported as mean ± SEM from *n* cells. Data distributions were tested for normality using the Shapiro-Wilk normality test. In case of non-parametric distribution Mann-Whitney test was applied to compare two groups. A one-way ANOVA was used for a comparison of means with multiple experimental conditions. Post-hoc analysis was performed using Fisher's least significant difference (LSD) test for statistical analysis of western blot data. Tukey's *post-hoc* test was used to assess statistical significance

of KPNA4 gain-of-function experiments. Nuclear-cytoplasmic ratios between w^{1118} and ΔNLS-TBPH larvae were assessed by unpaired *t*-tests. $p<0.05$ was considered significant.

Results

Decreased KPNA4 protein levels in post-mortem spinal cord of TDP-43-positive sALS

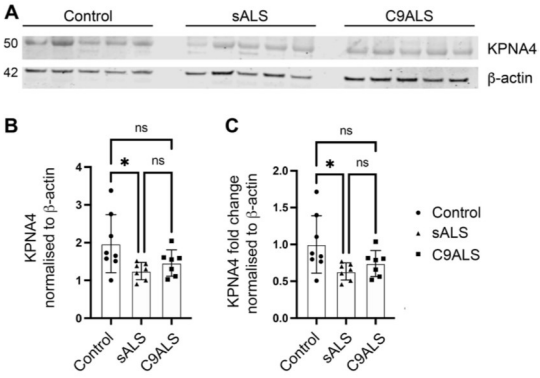

To determine whether KPNA4 abnormalities characterise ALS, we analysed the level and localisation of KPNA4 in post-mortem spinal cord of TDP-43-positive familial and sporadic cases. We first carried out semi-quantitative western blot analysis on human post-mortem samples to determine if KPNA4 levels varied between healthy, age-matched controls and sALS or C9ALS patients. sALS cases were found to have a significant decrease ($p = 0.0371$) in KPNA4 levels compared to age-matched controls (Figure). No significant changes were observed between any other groups. However, KPNA4 levels in C9ALS trended towards a decreased level ($p = 0.167$) when compared to controls, albeit less than sporadic individuals. Together these data suggest that KPNA4 levels are significantly reduced in post-mortem spinal cord of sporadic ALS cases that are associated with TDP-43 abnormalities.

Cytoplasmic mislocalisation of KPNA4 in post-mortem spinal cord of TDP-43-positive sALS and C9ALS

Next, we investigated whether KPNA4 pathology may extend to KPNA4 mislocalisation in spinal cord of sALS and C9ALS patient cases with TDP-43 pathology (Figure). To determine the cellular localisation of KPNA4, DAB conjugated immunohistochemistry of KPNA4 was performed on 22 post-mortem spinal cord samples obtained from 5 control cases (2 females and 3 males; mean ± SD age 66.4 ± 9 years), 8 sALS cases (4 females and 4 males; mean ± SD age 61.4 ± 9 years) and 9 C9ALS cases (4 females and 5 males; mean ± SD age 73.7 ± 10.8 years), summarized in Table 1. Samples were scored based on a semi-quantitative scale for anti-KPNA4 immunoreactivity to assess overall motor neuron staining, neuronal nuclear staining, the severity of reduced nuclear staining and neuronal cytoplasmic staining (detailed results can be provided upon request).

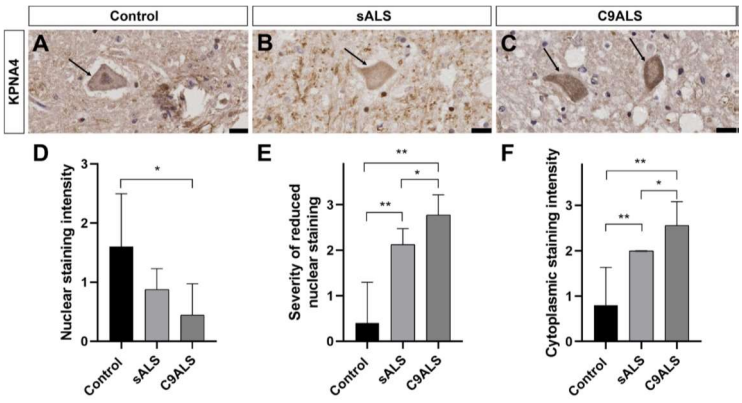

KPNA4 immunoreactivity in control cases predominantly displayed nuclear expression with minimal cytoplasmic immunolabelling (Fig. 2A). Of the control cases, nuclear KPNA4 immunolabelling was always observed, except for one case (tissue BBN_22594; Table 2) which revealed reduced nuclear expression that was variable amongst detectable motor neurons. In comparison, immunohistochemical analysis in both sporadic ALS (Fig. 2B) and C9ALS (Fig. 2C) cases revealed decrease of nuclear KPNA4 that was markedly pronounced in cases of C9ALS (Fig.

2D, E). Of note, one sALS case was an exemption to this pattern and displayed severely reduced KPNA4 nuclear staining that to some extent mimicked the situation observed for C9ALS cases (tissue BBN_22631; Table 2). In addition to its nuclear decrease, increased cytoplasmic expression of KPNA4 was detectable in C9ALS cases as recorded in the semi-quantitative assessment of neuronal cytoplasmic staining (Fig. 2F). No dystrophic neurites or inclusions were observed in any post-mortem spinal cord samples. Although, one possible skein-like inclusion may have been observed in a case of C9ALS (BBN_6254). Together these data identify KPNA4 pathology in TDP-43-positive ALS patient post-mortem spinal cord that is characterised by reduced protein levels of KPNA4 and its nuclear decrease, cellular phenotypes that in C9ALS cases are also accompanied by cytoplasmic mislocalisation of KPNA4.

Nuclear localisation signal-dependent interaction between TDP-43 and KPNA4

The majority of sporadic and familial ALS cases are characterised by TDP-43 pathology, especially its cytoplasmic mislocalisation and nuclear depletion[10]. Previous studies showed that TDP-43 can bind karyopherins *in vitro,* including KPNA4[30], suggesting that KPNA4 and TDP-43 pathologies might be functionally interlinked. To gain insights into the mechanistic link between TDP-43 and KPNA4 pathologies, we first determined whether TDP-43 interaction with KPNA4 occurs under physiological conditions.

We therefore performed a proximity biotinylation assay using biotin ligase 2 (BioID2) in human Flp-In HEK293 cell lines expressing control BioID2, or human TDP-43 in either its wildtype form (BioID2-TDP-43wt) or with its nuclear localisation signal deleted (BioID-TDP-43-dNLS). Subsequent pulldown using BioID2 as bait followed by immunostaining revealed interaction between KPNA4 and TDP-43 that was dependent on its nuclear localisation signal (Figure; red arrows). In contrast, no interaction was detected between TDP-43 and KPNA1, KPNA3, KPNA6 and KPNA7 (Fig. 3). While the de tection signal in whole lysate was weak for KPNA1 and KPNA3, a robust signal was observed for KPNA6 and KPNA7 (Figure, arrows). Together these data identify selective interaction between KPNA4 and TDP-43 that is dependent on its nuclear localisation signal.

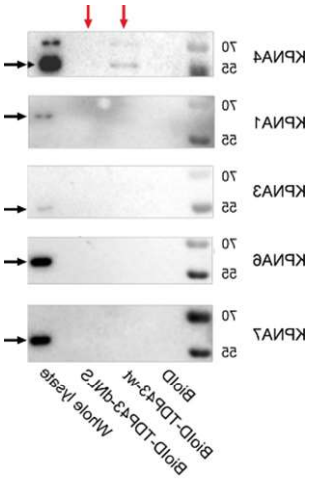

Targeted accumulation of *Drosophila* KPNA4 does not cause TDP-43 pathology

The observed phenotypes raise the question whether KPNA4 abnormalities are the cause or consequence of TDP-43 pathology. To address this, we turned to an *in vivo* animal model, *Drosophila melanogaster*, that has been successfully used to investigate cellular and molecular mechanisms related to ALS pathogenesis[40,41]. We utilised the Gal4/UAS system[42] for targeted expression and disease-related accumulation of the *Drosophila* homologue of KPNA4, karyopherin-α3 (Kap-α3) also named Importin-α3 (Imp-α3)[43].

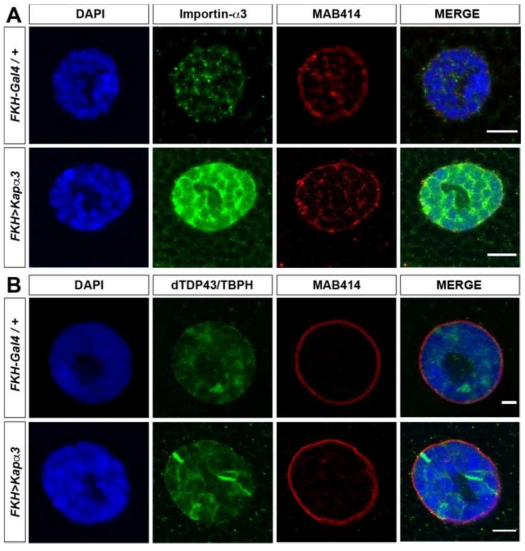

To investigate its effect on the nuclear-cytoplasmic localisation of the *Drosophila* TDP-43 homolog TBPH[38], we used the *FKH-Gal4* driver to misexpress

UAS-Kap-α3 in salivary gland cells that are large in diameter with a distinct nuclear to cytoplasm ratio that can be readily assessed[18]. To distinguish between the nucleus and cytoplasm, we co-immunolabelled with DAPI (nuclear stain) and anti-MAB414 which recognizes the conserved FG repeat sequence in nucleoporins[44]. Immunolabelling of anti-Importin-α3 in *FKH>Kap-α3* flies revealed an increase in nuclear expression but also accumulation of *Kap-α3* within the cytoplasm when compared to *FKH/+* controls (Figure A). However, immunolabelling of anti-TBPH revealed that Kap-α3 accumulation was insufficient to induce cytoplasmic mislocalisation of *Drosophila* TDP-43 (Figure B), suggesting that KPNA4 accumulation does not initiate TDP-43 pathology.

Cytoplasmic accumulation of *Drosophila* TDP-43 causes KPNA4 pathology

Next, we investigated whether KPNA4 abnormalities are a consequence of TDP-43 pathology. To address this, we expressed *Drosophila* TDP-43 with a mutated nuclear localisation signal (TBPH-ΔNLS) under control of the endogenous promotor for *TBPH*[18]. When compared to w^{1118} flies that control for the same genetic background as *TBPH-ΔNLS* flies, anti-TBPH immunolabelling revealed cytoplasmic accumulation of fly TDP-43 (Figure). To quantify such observations, mean pixel intensities were used to determine nuclear-cytoplasmic ratios. Assessment of the nuclear-cytoplasmic ratio revealed that expression of TBPH-ΔNLS resulted in cytoplasmic mislocalisation of TBPH, as well as its partial nuclear loss, when compared to w^{1118} control flies (Figure; unpaired *t*-test: ****P<0.0001). However, TBPH was not completely lost from the nucleus (Fig. 5A, B), since the TBPH-ΔNLS construct is expressed alongside two copies of endogenous wildtype TBPH protein harbouring an intact NLS which can still be recognised and thus enable nucleocytoplasmic transport.

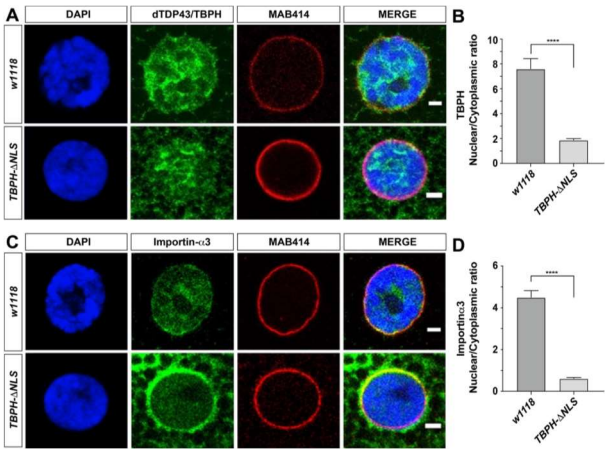

Subsequent anti-Importin-α3 immunolabelling revealed that ΔNLS-mediated accumulation of cytoplasmic TBPH induced the cytosolic mislocalisation and significant nuclear loss of the KPNA4 homologue, Imp-α3/Kap-α3, when compared to w^{1118} control flies (Fig. 4C, D; unpaired *t*-test: ****P<0.0001). Interestingly, a comparison of MAB414 immunolabelling between w^{1118} control and *TBPH-ΔNLS* genotypes indicated an unaltered pattern of expression of MAB414-recognised nuclear pore proteins[44], suggesting that the NPC remained intact and unaltered at this stage in the presence of accumulating *Drosophila* TDP-43. Together these data demonstrate that cytoplasmic accumulation of TDP-43 is sufficient to induce KPNA4 pathology, and not vice versa, suggesting that karyopherin abnormalities do not initiate but may contribute to the onset and progression of TDP-43-related pathogenesis.

Targeted gain of KPNA4 function partially restores its nuclear localisation in the presence of accumulating cytosolic TDP-43

To test whether karyopherin abnormalities may contribute to TDP-43 pathology, we first determined the potential to rescue KPNA4 phenotypes by targeted expression of *UAS-Kap-α3* in the presence of accumulating TDP-43. Thus, *ΔNLS; FKH>Kap-α3* flies were immunolabelled with anti-Imp-α3 and compared to w^{1118} and *FKH/+* controls as well as against *TBPH-ΔNLS* flies that show nuclear decrease and cytoplasmic accumulation of *Drosophila* KPNA4 (Figure A). Quantitative assessment revealed Kap-α3 overexpression increased the

nuclear ratio of Importin-α3 in *FKH>Kap-α3* flies (Figure B), as compared to control background (*FKH/+* control vs *FKH>Kap-α3*; Tukey *t*-test: p=0.0068), suggesting that targeted manipulation of *Drosophila* KPNA4 can direct its gain of function in nuclear-cytoplasmic transport.

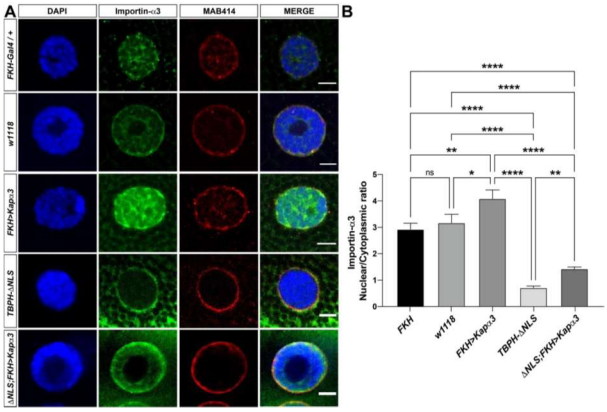

Importantly, significant differences in the nuclear-cytoplasmic ratio of Importin-α3 were detected across all experimental genotypes (one-way ANOVA: F= 76.23, p<0.0001) (Fig. 6B). Nuclear expression of Imp-α3 was more than 3 times greater in control backgrounds compared to *TBPH-ΔNLS* flies (Tukey t-test: p<0.0001 vs w^{1118}). Of note, upregulation of *Drosophila* KPNA4 led to an overall increase in its nuclear expression and partially rescued the pathological KPNA4 phenotype seen in *ΔNLS; FKH>Kap-α3* flies, when compared to *TBPH-ΔNLS* flies (Figure A, B; Tukey *t*-test: p= 0.0012) which was markedly lower than in both *FKH/+* and w^{1118} controls (Figure A, B; Tukey *t*-test: p<0.0001). These data suggest that targeted manipulation of KPNA4 increases its net translocation into the nucleus, which could be of beneficial effect to enhance KPNA4-dependent cargo transport. Since KNPA4 exhibits the strongest interaction among KPNAs with TDP-43[30], our data indicate that targeted gain of KPNA4 function might be able to counteract the cytosolic accumulation of its cargo TDP-43 which characterises the onset and progression of TDP-43 proteinopathies[10].

<u>Targeted gain of KPNA4 function partially rescues cytoplasmic mislocalisation and nuclear depletion of *Drosophila* TDP-43</u>

We thus determined whether targeted gain of KPNA4 function might be able to rescue, at least to some extent, TDP-43 mislocalisation in our fly model of TDP proteinopathy. *ΔNLS; FKH>Kap-α3* flies were immunolabelled with anti-TBPH (Fig. 7A) and the expression pattern was compared against w^{1118} and *FKH/+* controls, as well as against *FKH>Kap-α3* and *TBPH-ΔNLS* to investigate their impact on the nuclear-cytoplasmic ratio of TBPH (Fig. 7B). Qualitative assessment of high-resolution confocal images indicated that Kap-α3 overexpression affects the levels of cytoplasmic TBPH. Indeed, quantitative assessment of the nuclear-cytoplasmic ratio of TBPH revealed statistical significance between all genotypes (Figure; one-way ANOVA: F= 55.08, p<0.0001), suggesting that the nuclear-cytoplasmic localisation of *Drosophila* TDP-43 can be directed both ways.

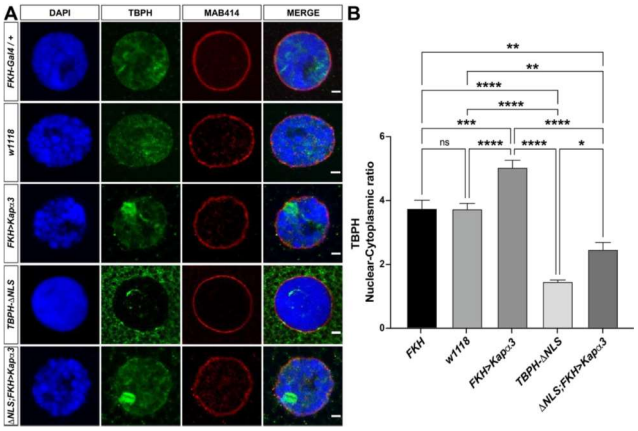

TBPH-ΔNLS flies exhibited a pronounced cytoplasmic mislocalisation of TBPH together with a decrease of its nuclear expression that was more than twofold lower when compared to w^{1118} controls (Figure; Tukey *t*-test: p<0.0001). Importantly, *FKH>Kap-α3* flies revealed a significantly enhanced nuclear-cytoplasmic ratio of TBPH compared to *FKH/+* controls (Fig. 7B; Tukey *t*-test: p =0.0001), suggesting that gain of KPNA4 function

was able to enhance TDP-43 cargo transport into the nucleus. Indeed, *ΔNLS; FKH>Kap-α3* flies immunolabelled with anti-TBPH revealed a nuclear-cytoplasmic ratio significantly greater than in *TBPH-ΔNLS* flies (Fig. 7B; Tukey *t*-test: p= 0.0398); but, noticeably lower than both *FKH/+* and w^{1118} controls (Figure ; Tukey *t*-test: p<0.01). Since TBPH-ΔNLS is expressed alongside two copies of endogenous wildtype TBPH with intact NLS, these data suggest that targeted manipulation of KPNA4 can increase cargo transport into the nucleus which counteracts the cytosolic accumulation and nuclear depletion of *Drosophila* TDP-43.

Discussion

Our results establish TDP-43 and KPNA4 abnormalities in post-mortem human spinal cord of both, sporadic ALS and C9ALS cases. KPNA4 pathology is characterised by reduced levels of soluble protein in conjunction with its nuclear decrease and cytoplasmic accumulation. KPNA4 selectively interacts with TDP-43 which is dependent on its nuclear localisation signal. *In vivo* analysis in *Drosophila* revealed that KPNA4 abnormalities can be induced by accumulating cytoplasmic TDP-43, whereas overexpression of KPNA4 is insufficient to cause TDP-43 pathology. Targeted gain of KPNA4 function restored nuclear KPNA4 in the presence of accumulating cytoplasmic TDP-43 and was able to partially rescue the nuclear depletion of TDP-43. These findings identify a direct feedback loop between TDP-43 dysfunction and KPNA4 abnormalities, with implications for understanding the pathogenesis and targeted treatment of TDP-43 proteinopathies.

Impaired nucleocytoplasmic transport including Karyopherin abnormalities characterise ALS and FTD

Previous studies identified KPNA4 pathology in post-mortem human frontal cortex of sporadic FTD and C9FTD cases that also showed TDP-43 pathology[18,27]. These cases were characterised by reduced levels of soluble protein together with nuclear decrease and cytoplasmic accumulation of KPNA4[18]. Our findings presented here establish corresponding phenotypes in post-mortem human spinal cord of TDP-43-positive sporadic ALS and C9ALS cases. Of note, concomitant western blot and immunohistochemical analyses confirmed the observed alterations in protein level are not merely due to the loss of neurons within the spinal cord of the investigated sALS and C9ALS cases. Together with our earlier observations restricted to FTD[18], the findings presented here identify KPNA4 pathology as a common denominator of both ALS and FTD with TDP-43 pathology. This data, however, does not exclude the possibility that karyopherins other than KPNA4 are also affected, as has been shown for KPNA2 in FTD-TDP[18,30] as well as for KPNA2 and KPNA6 in ALS[30]. However, our BioID experiments demonstrate a selective interaction between TDP-43 and KPNA4 that was not detected for KPNA1, KPNA3, KPNA6 and KPNA7. Together these findings suggest a direct link between TDP-43 and KPNA4 pathology in TDP-43 proteinopathies.

TDP-43 proteinopathies are characterised by the cytoplasmic accumulation and nuclear depletion of TDP-43. While the origin and initiating cause of cytosolic TDP-43 accumulation remain enigmatic, recent studies identified nucleocytoplasmic transport deficits as a key pathogenic mechanism involved in ALS and FTD, especially in C9ALS/FTD[45-47]. These studies revealed that karyopherins, in particular importins directly bind arginine-rich DPRs[28,33,48] and are sequestered into cytoplasmic inclusions by aggregating β-sheet proteins, including fragments of TDP-43, and poly-GA[49,50]. Moreover, arginine-rich DPRs can perturb karyopherin-β (KPNB)-related cargo-loading in a dose- and length- dependent manner[48] or promote importin insolubility and condensation that impair nuclear import of TDP-43[33]. While these findings provide further evidence for a direct link between TDP-43 dysfunction and karyopherin abnormalities[29], it has remained elusive whether these defects in

nucleocytoplasmic transport are a consequence or rather contribute to TDP-43 pathology[47]. We now present evidence in *Drosophila* suggesting that TDP-43 pathology precedes KPNA4 abnormalities and not vice versa, indicating that both converge in the onset and progression of disease.

Concurrent TDP-43 and KPNA4 pathology

Our findings in *Drosophila* provide experimental evidence that accumulating cytosolic TDP-43 causes the nuclear decrease and cytoplasmic accumulation of KPNA4, cellular phenotypes that characterise KPNA4 pathology seen in the brain of FTD and spinal cord of ALS patients. In contrast, targeted overexpression of KPNA4 was insufficient to cause cytoplasmic accumulation and nuclear depletion of TDP-43. These data imply that karyopherin abnormalities are a consequence of, rather than initiate the cytoplasmic accumulation of TDP-43. Instead, our data suggest that an initially modest mislocalisation of TDP-43 can impair the levels and localisation of KPNA4 which in turn impairs nuclear transport, thereby leading to a feedback loop that further impacts the localisation of TDP-43 as well as nucleocytoplasmic transport in general[18]. According to this model, the resulting nucleocytoplasmic transport deficit further exacerbates cytosolic accumulation of TDP-43 and as a secondary consequence also impairs the NPC[18]. Consistent with this model, in our study expression of ΔNLS-TBPH was sufficient to induce cytoplasmic mislocalisation and nuclear decrease of KPNA4 in the early absence of nuclear pore complex pathology, as indicated by an unaltered expression pattern of MAB414 that recognizes the conserved FG motif in nuclear pore proteins Nup62, Nup153, Nup214 and Nup358[44].

Furthermore, our feedback model predicts that karyopherin abnormalities concur with accumulating cytosolic TDP-43 which in turn cause its nuclear depletion seen in TDP-43 proteinopathies[10]. These predictions are in line with previous studies in primary neurons and transgenic mice, in which expression of human TDP-43 with a defective NLS decreased endogenous mouse TDP-43 levels that was accompanied by the accumulation of cytoplasmic TDP-43 and the nuclear clearance of endogenous TDP-43[15,16]. Of note, reversible expression of human ΔNLS-TDP-43 in mice recapitulated these phenotypes, whereas the subsequent removal of cytoplasmic TDP-43 led to return of nuclear TDP-43 and functional recovery[17]. These data imply shuttling across the nuclear pore is not only an essential requirement for the localisation and function of TDP-43 but also sufficient to prevent its cytoplasmic accumulation on condition that a functional NLS is present for karyopherin binding and cargo transport[10]. Indeed, our results demonstrate that targeted gain of KPNA4 in *Drosophila* shifted the nucleo-cytoplasmic ratio of both, KPNA4 (Fig. 6B) and TDP-43 (Fig. 7B) towards the nucleus in *FKH>Kap-α3* flies, indicating that excess KPNA4 not only shuttled increasingly into the nucleus but also together with its cargo TDP-43. This interpretation is consistent with previous studies which established among karyopherins that KPNA4 features the strongest interaction with TDP-43, and that an intact NLS is essential for karyopherin binding of TDP-43 (Fig. 3). Together these data suggest that karyopherin gain of function might be of therapeutic value for targeting TDP-43 proteinopathies.

Targeting nucleocytoplasmic transport and karyopherin function in TDP-43 proteinopathies

Our experiments in *Drosophila* employed a gain-of-function mechanism of the KPNA4 homologue Importin-α3 to target the nuclear decrease of KPNA4 itself and that of TDP-43. We observed KPNA4 is necessary and sufficient for nuclear import of TDP-43 and that upregulation of fly KPNA4 led to a partial rescue and nuclear restoration of TDP-43 despite its concurrent accumulation within the cytoplasm. The fact that we only observed a partial rescue could be attributed to at least two possible impeding circumstances. Shuttling of TDP-43 has

been reported to involve both KPNA and KPNB1 which together form a trimeric complex that mediates nuclear import of TDP-43[51]. Thus, gain of KPNA4 function on its own might be insufficient for a complete rescue but instead would require a gain of function mechanism including both KPNA4 and KPNB1. However, a recent study[52] suggests this may not be the case. These experiments determined the cytoplasmic/nuclear ratio of *Drosophila* TBPH in C4da neurons which revealed that ratios differed only slightly between Imp-α3/KPNA4 overexpression on its own and the concomitant overexpression of Imp-α3 together with Imp-β1/KPNB1[52]. In comparison to what we observed, these data suggest the lack of KPNB1 in our gain of function experiments may account for only a small part of the incomplete rescue of the detected TDP-43 pathology.

Instead, the observed incomplete rescue might be accountable in large parts to the continued expression of *Drosophila* TDP-43 without a functional NLS (TBPH-ΔNLS) alongside two copies of endogenous wildtype TBPH. Since karyopherin binding of TDP-43 requires an intact NLS, our results indicate that gain of KPNA4 function was only able to target endogenous wildtype TBPH which was sufficient to shift the nucleo-cytoplasmic ratio of TDP-43 towards the nucleus even in the presence of continuously produced TBPH-ΔNLS. These data imply that targeting KPNA4 can restore TDP-43 cargo transport into the nucleus and thus counteract its nuclear depletion triggered by accumulating cytoplasmic TDP-43. However, such a gain of karyopherin function is insufficient to target TDP-43 without a functional NLS, a limitation that also applies to the C-terminal fragments of TDP-43 that are commonly observed in familial and sporadic forms of ALS and FTD[6,7]. Nevertheless, this does not invalidate the therapeutic potential of targeting karyopherin function in TDP-43 proteinopathies. Familial cases are heterozygous for mutation of TDP-43. Thus, a functional TDP-43 wildtype copy with intact NLS is also expressed and available for karyopherin-mediated nuclear import. Similarly, sporadic cases also express functional wildtype copies of TDP-43[10]. It is therefore reasonable to suggest that targeting karyopherin function might be a potent therapeutic strategy[29] to counteract the cytosolic accumulation and subsequent nuclear depletion of TDP-43, which in turn could sustain minimum levels of nuclear TDP-43 that are essential for cellular homeostasis and neuronal function affected in neurodegenerative disease.

References

1. Hardiman O, Al-Chalabi A, Brayne C et al The changing picture of amyotrophic lateral sclerosis: lessons from European registers. *J Neurol Neurosurg Psychiatry* 2017;88:557-563. https://doi.org/10.1136/jnnp-2016-314495
2. Hortobagyi T, Cairns NJ. Amyotrophic lateral sclerosis and non-tau frontotemporal lobar degeneration. *Handb Clin Neurol.* 2017;145:369-381. https://doi.org/10.1016/B978-0-12-802395-2.00026-2
3. Renton AE, Chio A, Traynor BJ. State of play in amyotrophic lateral sclerosis genetics. *Nat Neurosci.* 2014;17(1):17-23. https://doi.org/10.1038/nn.3584
4. Lomen-Hoerth C, Anderson T, Miller B. The overlap of amyotrophic lateral sclerosis and frontotemporal dementia. *Neurology* 2002;59(7):1077-1079. https://doi.org/10.1212/wnl.59.7.1077
5. Van Langenhove T, van der Zee J, Van Broeckhoven C. The molecular basis of the frontotemporal lobar degeneration-amyotrophic lateral sclerosis spectrum. *Ann Med.* 2012;44(8):817-828. https://doi.org/10.3109/07853890.2012.665471
6. Arai T, Hasegawa M, Akiyama H et al. TDP-43 is a component of ubiquitin-positive tau-negative inclusions in frontotemporal lobar degeneration and amyotrophic lateral sclerosis. *Biochem Biophys Res Commun.* 2006;351(3):602-611. https://doi.org/10.1016/j.bbrc.2006.10.093
7. Neumann M, Sampathu DM, Kwong LK et al. Ubiquitinated TDP-43 in frontotemporal lobar degeneration and amyotrophic lateral sclerosis. *Science* 2006;314(5796): 130-133. https://doi.org/10.1126/science.1134108
8. Ling SC, Polymenidou M, Cleveland DW. Converging mechanisms in ALS and FTD: disrupted RNA and protein homeostasis. *Neuron* 2013;79(3):416-438. https://doi.org/10.1016/j.neuron.2013.07.033
9. Ayala YM *et al.* Human, Drosophila, and C. elegans TDP43: nucleic acid binding properties and splicing regulatory function. *J Mol Biol.* 2005; 348:575–588.
10. Tziortzouda P, Van Den Bosch L, Hirth F. Triad of TDP-43 control in neurodegeneration: autoregulation, localisation and aggregation. *Nat Rev Neurosci.* 2021;22(4):197-208. https://doi.org/10.1038/s41583-021-00431-1
11. Buratti, E. and F. E. Baralle (2008). Multiple roles of TDP-43 in gene expression, splicing regulation, and human disease. *Front Biosci* 13: 867-878. https://doi.org/10.2741/2727

12. Sreedharan J, Blair IP, Tripathi VB et al. TDP-43 mutations in familial and sporadic amyotrophic lateral sclerosis. *Science* 2008;319(5870):1668-1672. https://doi.org/10.1126/science.1154584
13. Kabashi E, Valdmanis PN, Dion P et al. TARDBP mutations in individuals with sporadic and familial amyotrophic lateral sclerosis. *Nat Genet.* 2008;40(5):572-574. https://doi.org/10.1038/ng.132
14. Yokoseki A, Shiga A, Tan CF et al. TDP-43 mutation in familial amyotrophic lateral sclerosis. *Ann Neurol.* 2008;63(4):538-542. https://doi.org/10.1002/ana.21392
15. Winton MJ, Igaz LM, Wong MM, Kwong LK, Trojanowski JQ, Lee VM. Disturbance of nuclear and cytoplasmic TAR DNA-binding protein (TDP-43) induces disease-like redistribution, sequestration, and aggregate formation. *J Biol Chem* 2008;283(19):.13302-13309. https://doi.org/10.1074/jbc.M800342200
16. Igaz LM, Kwong LK, Lee EB et al. Dysregulation of the ALS-associated gene TDP-43 leads to neuronal death and degeneration in mice. *J Clin Invest.* 2011;121(2):726-738. https://doi.org/10.1172/JCI44867
17. Walker AK, Spiller KJ, Ge G et al. Functional recovery in new mouse models of ALS/FTLD after clearance of pathological cytoplasmic TDP-43. *Acta Neuropathol* 2015;130(5):643-660. https://doi.org/10.1007/s00401-015-1460-x
18. Solomon DA, Stepto A, Au WH et al. A feedback loop between dipeptide-repeat protein, TDP-43 and karyopherin-alpha mediates C9orf72-related neurodegeneration. *Brain* 2018;141(10):2908-2924. https://doi.org/10.1093/brain/awy241
19. DeJesus-Hernandez M, Mackenzie IR, Boeve BF et al. Expanded GGGGCC hexanucleotide repeat in noncoding region of C9ORF72 causes chromosome 9p-linked FTD and ALS. *Neuron* 2011;72(2):245-256. https://doi.org/10.1016/j.neuron.2011.09.011
20. Renton, A. E., E. Majounie, A. Waite, J. Simon-Sanchez, S. Rollinson, J. R. Gibbs et al (2011). A hexanucleotide repeat expansion in C9ORF72 is the cause of chromosome 9p21-linked ALS-FTD. *Neuron* 72(2): 257-268. https://doi.org/10.1016/j.neuron.2011.09.010
21. Murray, M. E., M. DeJesus-Hernandez, N. J. Rutherford, M. Baker, R. Duara, N. R. Graff-Radford et al (2011). Clinical and neuropathologic heterogeneity of c9FTD/ALS associated with hexanucleotide repeat expansion in C9ORF72. *Acta Neuropathol* 122(6): 673-690. https://doi.org/10.1007/s00401-011-0907-y
22. Mori, K., S. M. Weng, T. Arzberger, S. May, K. Rentzsch, E. Kremmer et al (2013). The C9orf72 GGGGCC repeat is translated into aggregating dipeptide-repeat proteins in FTLD/ALS. *Science* 339(6125): 1335-1338. https://doi.org/10.1126/science.1232927
23. Freibaum BD, Lu Y, Lopez-Gonzalez R et al. GGGGCC repeat expansion in C9orf72 compromises nucleocytoplasmic transport. *Nature* 2015;525(7567):129-133. https://doi.org/10.1038/nature14974
24. Zhang K, Donnelly CJ, Haeusler AR et al. The C9orf72 repeat expansion disrupts nucleocytoplasmic transport. *Nature* 2015;525(7567):56-61. https://doi.org/10.1038/nature14973
25. Jovicic A, Mertens J, Boeynaems S et al. Modifiers of C9orf72 dipeptide repeat toxicity connect nucleocytoplasmic transport defects to FTD/ALS. *Nat Neurosci* 2015;18(9):1226-1229. https://doi.org/10.1038/nn.4085
26. Boeynaems S, Bogaert E, Michiels E et al. Drosophila screen connects nuclear transport genes to DPR pathology in c9ALS/FTD. *Sci Rep.* 2016;6:20877. https://doi.org/10.1038/srep20877
27. Chou CC, Zhang Y, Umoh ME et al (2018). TDP-43 pathology disrupts nuclear pore complexes and nucleocytoplasmic transport in ALS/FTD. *Nat Neurosci* 21(2): 228-239. https://doi.org/10.1038/s41593-017-0047-3
28. Lee KH, Zhang P, Kim HJ et al. C9orf72 Dipeptide Repeats Impair the Assembly, Dynamics, and Function of Membrane-Less Organelles. *Cell* 2016;167(3):774-788 e717. https://doi.org/10.1016/j.cell.2016.10.002
29. Pasha T, Zatorska A, Sharipov D, Rogelj B, Hortobagyi T, Hirth F. Karyopherin abnormalities in neurodegenerative proteinopathies. *Brain* 2021;144(10):2915-2932. doi: 10.1093/brain/awab201.
30. Nishimura AL, Zupunski V, Troakes C et al. Nuclear import impairment causes cytoplasmic trans-activation response DNA-binding protein accumulation and is associated with frontotemporal lobar degeneration. *Brain* 2010;133:1763-1771. https://doi.org/10.1093/brain/awq111
31. Gasset-Rosa F, Lu S,Yu H et al. Cytoplasmic TDP-43 De-mixing Independent of Stress Granules Drives Inhibition of Nuclear Import, Loss of Nuclear TDP-43, and Cell Death. *Neuron* 2019;102(2):339-357 e337. https://doi.org/10.1016/j.neuron.2019.02.038
32. Guo L, Kim HJ, Wang H et al. Nuclear-Import Receptors Reverse Aberrant Phase Transitions of RNA-Binding Proteins with Prion-like Domains. *Cell* 2018;173(3):677-692.e20. doi: 10.1016/j.cell.2018.03.002.
33. Hutten S, Usluer S, Bourgeois B et al. Nuclear Import Receptors Directly Bind to Arginine-Rich Dipeptide Repeat Proteins and Suppress Their Pathological Interactions. *Cell Rep.* 2020;33(12):108538. https://doi.org/10.1016/j.celrep.2020.108538
34. Cairns NJ, Neumann M, Bigio EH et al. TDP-43 in familial and sporadic frontotemporal lobar degeneration with ubiquitin inclusions. *Am J Pathol.* 2007;171(1):227-240. https://doi.org/10.2353/ajpath.2007.070182
35. Al-Sarraj, S., A. King, C. Troakes, B. Smith, S. Maekawa, I. Bodi et al (2011). p62 positive, TDP-43 negative, neuronal cytoplasmic and intranuclear inclusions in the cerebellum and hippocampus define the pathology of C9orf72-linked FTLD and MND/ALS. *Acta Neuropathol* 122(6): 691-702. https://doi.org/10.1007/s00401-011-0911-2
36. Sowa AS, Martin E, Martins IM et al. Karyopherin alpha-3 is a key protein in the pathogenesis of spinocerebellar ataxia type 3 controlling the nuclear localization of ataxin-3. *Proc Natl Acad Sci. USA* 2018;115(11):E2624-E2633. https://doi.org/10.1073/pnas.1716071115
37. Velentzas PD, Zhang L, Das G et al. The Proton-Coupled Monocarboxylate Transporter Hermes Is Necessary for Autophagy during Cell Death. *Dev Cell* 2018;47(3):281-293 e284. https://doi.org/10.1016/j.devcel.2018.09.015
38. Diaper DC, Adachi Y, Sutcliffe B et al. Loss and gain of Drosophila TDP-43 impair synaptic efficacy and motor control leading to age-related neurodegeneration by loss-of-function phenotypes. *Hum Mol Genet* 2013;22(8):1539-1557. https://doi.org/10.1093/hmg/ddt005
39. Diaper DC, Hirth F. Immunostaining of the developing embryonic and larval Drosophila brain. *Methods Mol Biol.* 2013;1082: 3-17. https://doi.org/10.1007/978-1-62703-655-9_1

40. Hirth F. Drosophila melanogaster in the study of human neurodegeneration. *CNS Neurol Disord Drug Targets* 2010;9(4):504-523. https://doi.org/10.2174/187152710791556104
41. Casci I, Pandey UB. A fruitful endeavor: modeling ALS in the fruit fly. *Brain Res.* 2015;1607:47-74. https://doi.org/10.1016/j.brainres.2014.09.064
42. Brand AH, Perrimon N. Targeted gene expression as a means of altering cell fates and generating dominant phenotypes. *Development* 1993;118(2):401-415.
43. Mason DA, Goldfarb DS (2009). The nuclear transport machinery as a regulator of Drosophila development. *Semin Cell Dev Biol.* 2009;20(5):582-589. https://doi.org/10.1016/j.semcdb.2009.02.006
44. Davis LI, Blobel G. Nuclear pore complex contains a family of glycoproteins that includes p62: glycosylation through a previously unidentified cellular pathway. *Proc. Natl. Acad. Sci. USA* 1987;84(21):7552-7556. https://doi.org/10.1073/pnas.84.21.7552
45. Boeynaems S, Bogaert E, Van Damme P, Van Den Bosch L. Inside out: the role of nucleocytoplasmic transport in ALS and FTLD. *Acta Neuropathol.* 2016;132(2):159-173. https://doi.org/10.1007/s00401-016-1586-5
46. Kim HJ, Taylor JP. Lost in Transportation: Nucleocytoplasmic Transport Defects in ALS and Other Neurodegenerative Diseases. *Neuron* 2017;96(2):285-297. https://doi.org/10.1016/j.neuron.2017.07.029
47. Hutten S, Dormann D. Nucleocytoplasmic transport defects in neurodegeneration - Cause or consequence? *Semin Cell Dev Biol.* 2020;99:151-162. https://doi.org/10.1016/j.semcdb.2019.05.020
48. Hayes, L. R., L. Duan, K. Bowen, P. Kalab and J. D. Rothstein (2020). C9orf72 arginine-rich dipeptide repeat proteins disrupt karyopherin-mediated nuclear import. *Elife* 9. https://doi.org/10.7554/eLife.51685
49. Khosravi B, Hartmann H, May S et al. Cytoplasmic poly-GA aggregates impair nuclear import of TDP-43 in C9orf72 ALS/FTLD. *Hum Mol Genet* 2017;26(4):790-800. https://doi.org/10.1093/hmg/ddw432
50. Woerner, A. C., F. Frottin, D. Hornburg, L. R. Feng, F. Meissner, M. Patra et al (2016). Cytoplasmic protein aggregates interfere with nucleocytoplasmic transport of protein and RNA. *Science* 351(6269): 173-176. https://doi.org/10.1126/science.aad2033
51. Prpar Mihevc S, Darovic S, Kovanda A, Bajc Cesnik A, Zupunski V, Rogelj B. Nuclear trafficking in amyotrophic lateral sclerosis and frontotemporal lobar degeneration. *Brain* 2017;140(1):13-26. https://doi.org/10.1093/brain/aww197
52. Park JH, Chung CG, Park SS et al (2020). Cytosolic calcium regulates cytoplasmic accumulation of TDP-43 through Calpain-A and Importin alpha3. *Elife* 2020;9:e60132 https://doi.org/10.7554/eLife.60132

3. The role of karyopherin abnormalities in the onset and progression of synucleinopathies (Oral presentation by the PI`s (TH) PhD student Daulet Sharipov at the International Society of Neuropathology Conference, Berlin, September 2023)

Parkinson's Disease (PD), Dementia with Lewy Bodies (DLB), and Parkinson's Disease Dementia (PDD) are synucleinopathies characterised by the aggregation of alpha-synuclein (aSyn). aSyn is a disordered protein prone to accumulation via phase separation (PS). Previous studies showed that PS is associated with karyopherins (KPN), mediating nucleocytoplasmic cargo transport and acting as disaggregases against misfolding proteins. Furthermore, KPN abnormalities have been implicated in synucleinopathy, but their role in disease formation remains enigmatic.

Using a multi-disciplinary approach, we characterised levels and localisation of KPN and aSyn in the prefrontal cortex (BA9) of human post-mortem brain tissue of controls, Alzheimer's Disease (AD), PD, DLB and PDD. We also used human SH-SY5Y cells and *Drosophila* for accumulation of either wildtype or mutant (A30P) aSyn and established its effect on KPNs.

Our analyses identified altered KPN expression levels in BA9 that were not detected in AD nor controls. We found aSyn accumulated and aggregated in the cytoplasm and nucleus, with an altered nucleocytoplasmic ratio in BA9 of the investigated cases versus controls. Moreover, KPN was depleted from the cytoplasm and accumulated in the nucleus in PD, PDD and DLB, with abnormal nuclear co-localisation with aSyn. New *Drosophila* models of synucleinopathy demonstrated that accumulating aSyn caused alterations in levels and localisation of KPN and progressive motor impairment that were exacerbated by aSyn-A30P. Human cell experiments revealed that accumulating aSyn-A30P formed spontaneous intracellular aggregates that sequestered and mislocalised KPN, a pathogenic process accelerated in the presence of prefibrillar aSyn.

Overall, our findings demonstrate the pathological accumulation of nuclear aSyn and KPN alterations in PD, PDD and DLB, suggesting a vicious cycle of protein alterations that propagate the pathological aggregation of aSyn in neurodegenerative synucleinopathies. (Manuscript in preparation. More detailed results are available upon request.)

4. **Comparison of semi-quantitative scoring and artificial intelligence aided digital image analysis of chromogenic immunohistochemistry.** (Bencze J., Szarka M., Kóti B., Seo W., Hortobágyi T.G., Bencs V., Módis L.V., Hortobágyi T.: Comparison of semi-quantitative scoring and artificial intelligence aided digital image analysis of chromogenic immunohistochemistry. Biomolecules. 2022; 12:19.) (See paper 5 in the publication list below)

This is a methodological paper, which addressed one of the aims of the grant to use computer-assisted image analysis. It has been applied in Alzheimer`s disease human post-mortem material and can be applied in future publications also in TDP-43 proteinopathies (FTD/ALS) also for analysis of nuclear transport abnormalities. The summary of the paper is as follows:

Semi-quantitative scoring is a method that is widely used to estimate the quantity of proteins on chromogen-labelled immunohistochemical (IHC) tissue sections. However, it suffers from several disadvantages, including its lack of objectivity and the fact that it is a time-consuming process. Our aim was to test a recently established artificial intelligence (AI)-aided digital image analysis platform, Pathronus, and to compare it to conventional scoring by five observers on chromogenic IHC-stained slides belonging to three experimental groups. Because Pathronus operates on grayscale 0-255 values, we transformed the data to a seven-point scale for use by pathologists and scientists. The accuracy of these methods was evaluated by comparing statistical significance among groups with quantitative fluorescent IHC reference data on subsequent tissue sections. The pairwise inter-rater reliability of the scoring and converted Pathronus data varied from poor to moderate with Cohen's kappa, and overall agreement was poor within every experimental group using Fleiss' kappa. Only the original and converted that were obtained from Pathronus original were able to reproduce the statistical significance among the groups that were determined by the reference method. In this study, we present an AI-aided software that can identify cells of interest, differentiate among organelles, protein specific chromogenic labelling, and nuclear counterstaining after an initial training period, providing a feasible and more accurate alternative to semi-quantitative scoring.

Of note, in a previous paper (No. 5 in the list below) also acknowledging the NKFIH grant a quantitative digital analysis of immunofluorescent signals has been introduced, as a relevant methodological advancement in our research team (Bencze J., et al., Hortobágyi T.: Lemur tyrosine kinase 2 (LMTK2) level inversely correlates with phospho-tau in neuropathological stages of Alzheimer's disease Brain Sciences. 2020; 10; 68 (13 pages)).

5. **List of Manuscripts/Publications with acknowledgement of grant NKFIH-SNN 132999.** The 3 papers which are closely related to grant (outlined above at subheadings 1, 2 and 4) are set with `italics` font type. Sum of Impact Factor: 52,768

Publications in progress**:**

1. Fekete R., Simats A., Bíró E., Cserép C., Schwarcz A.D., Pósfai B., Szabadits E., Környei Z., Tóth K., Kellermayer A., Dávid C., Acsády L., Kontra L., Silvestre-Roig C., Moldvay

J., Fillinger J., Hortobágyi T., Liesz A., Benkő S., Dénes Á.: Infection-induced vascular inflammation in COVID-19 links focal microglial dysfunction with neuropathologies through IL-1/IL-6-related systemic inflammatory states.
bioRxiv. *2023.06.23.546214. doi: https://doi.org/10.1101/2023.06.23.546214*
(under review in a D1/Q1 journal)

2. Sárkány B., Dávid C., Hortobágyi T., Gombás P., Somogyi P.,[1] Acsády L., Viney T.J.: Early and selective subcortical Tau pathology within the human Papez circuit.
bioRxiv. *2023.06.05.543738. doi: https://doi.org/10.1101/2023.06.05.543738*
(under review in a D1/Q1 Journal)

3. *Atwal M.S., Carre I., Tziortzouda P., Čerček U., Zatorska A., Pasha T., Mitchell J., Troakes C., Župunski V., Rogelj B., Hortobágyi T., Hirth F.: A Pathogenic Feedback Loop between TDP-43 and Karyopherin-α4 in Amyotrophic Lateral Sclerosis.*
(prepared for submission to a D1/Q1 journal)

Full Papers:

2022

4. Varkoly G., Hortobágyi T.G., Gebri E., Bencze J, Hortobágyi T., Módis L. Jr.: Expression Pattern of Tenascin-C, Matrilin-2, and Aggrecan in Diseases Affecting the Corneal Endothelium.
Journal of Clinical Medicine. *2022; 11:5991. doi: 10.3390/jcm11205991.*
IF: 3.9, Q2

5. *Bencze J., Szarka M., Kóti B., Seo W., Hortobágyi T.G., Bencs V., Módis L.V., Hortobágyi T.: Comparison of semi-quantitative scoring and artificial intelligence aided digital image analysis of chromogenic immunohistochemistry.*
Biomolecules. *2022; 12:19. https://doi.org/10.3390/biom12010019*
IF: 5.5, Q1

2021

6. *Pasha T., Zatorska A., Sharipov D., Rogelj B., Hortobágyi T., Hirth F.: Karyopherin abnormalities in neurodegenerative proteinopathies.*
Brain. *2021; 144:2915-32; doi: 10.1093/brain/awab201.doi: 10.1093/brain/awab201.*
IF: 15.255, D1/Q1

7. Attems J., Toledo J.B., Walker L., Gelpi E., Gentleman S., Halliday G., Hortobágyi T., Jellinger K., Kovacs G.G., Lee E.B., Love S., McAleese K.E., Nelson P.T., Neumann M., Parkkinen L., Polvikoski T. Sikorska B., Smith C., Tenenholz Grinberg L., Thal D.R., Trojanowski J.Q., McKeith I.G.: Neuropathological consensus criteria for the evaluation of Lewy pathology in post-mortem brains; a multi-centre study.
Acta Neuropathologica. *2021; 141:159-172. doi: 10.1007/s00401-020-02255-2*
IF: 15.887, D1/Q1

8. Gebri E., Kiss A., Tóth F., Hortobágyi T.: Salivary Osteopontin as a potential biomarker for oral mucositis.
Metabolites. *2021;11:208. doi: 10.3390/metabo11040208.*
IF: 5.581, Q2

9. Módis L.V. *, Varkoly G. *, Bencze J., Hortobágyi T.G., Módis L. Jr**, Hortobágyi T. **: Extracellular matrix changes in corneal opacification vary depending on etiology.
Molecular Vision. *2021; 27:26-36. http://www.molvis.org/molvis/v27/26*
IF: 2,711, Q3

2020

10. Bencs V., Bencze J., Módis V.L., Simon V., Kálmán J., Hortobágyi T.: Clinicopathological comparison of Parkinson's Disease Dementia and Dementia with Lewy bodies. (A Parkinson-kórhoz társuló demencia és a Lewy-testes demencia klinikopatológiai összehasonlítása)(in Hungarian)
Orvosi Hetilap/Hungarian Medical Journal. 2020; 161:727-737.
IF: 0.54, Q4

11. Bencze J., Seo W., Hye A., Aarsland D., Hortobágyi T.: Dementia with Lewy bodies – a clinicopathological update.
Free Neuropathology. *2020; 1:7 (12 pages) https://doi.org/10.17879/freeneuropathology-2020-2613*
IF: New journal

12. Bencze J., Szarka M., Bencs V., Szabó R.N., Módis L.V., Aarsland D., Hortobágyi T.: Lemur tyrosine kinase 2 (LMTK2) level inversely correlates with phospho-tau in neuropathological stages of Alzheimer's disease
Brain Sciences. 2020; 10; 68 (13 pages). https://doi.org/10.3390/brainsci10020068
IF: 3.394, Q3